BOLLETTINO DI GEOFISICA TEORICA ED APPLICATA VOL. 42, N. 1-2, PP. 41-55; MAR.-JUN. 2001

Parametric-historic procedure for seismic hazard assessment and its application to northern Europe

P. MÄNTYNIEMI(1), A. KIJKO(2) and P. RETIEF(2)

(1) *Institute of Seismology, University of Helsinki, Finland*
(2) *Council for Geoscience, South Africa*

(Received February 15, 2001; accepted June 4, 2001)

Abstract - A new methodology for probabilistic seismic hazard assessment is outlined and applied to parts of the northern European intraplate. The purpose is to gain more experience of the applicability of the technique to low-seismicity areas, where probabilistic seismic hazard assessment is often difficult because of a sparseness of data. The new technique is free from the subjective judgement involved in identifying seismogenic source zones, when specific active faults have not been mapped and where the causes of seismicity are not fully understood, and it takes into account the incompleteness of available earthquake catalogues and the error of earthquake magnitudes. Two cases are presented, in which seismic hazard is estimated for a specified site and a seismic hazard map is generated for a larger region. It was found that the methodology is very advantageous for investigating regions of low and moderate seismicity.

1. Introduction

Probabilistic seismic hazard assessment (PSHA) is performed using a variety of methodologies to quantify the seismic potential in given areas. It is obvious that regions of high seismicity such as plate margins receive most of the attention in this field. A high seismic activity rate also means that different kinds of information are usually available for PSHA input such as records of historical and instrumental seismicity, strong motion databases, geologic and tectonic information and recognition of individual active faults.

Much of the work on PSHA for low-seismicity regions, e.g. plate interiors, during the past few decades was motivated by the needs of modern societies, as the level of seismic hazard in areas of low to moderate seismicity may pose a threat to critical structures. In most cases these

Corresponding author: P. Mäntyniemi, Institute of Seismology, University of Helsinki, P.O. Box 26 (Teollisuuskatu 23), FIN-00014 Helsinki, Finland; phone: +358919144447; fax: +358919144430; e-mail: paivi@seismo.helsinki.fi

efforts were site-specific. However, the Global Seismic Hazard Assessment Program (GSHAP) during the 1990s demonstrated the need for accurate hazard mapping also for regions of low seismicity (cf. Giardini and Basham, 1993; Grünthal and the GSHAP Region 3 Working Group, 1999). New evidence of earthquakes in stable continental regions also need be incorporated into mapping practice (e.g., Adams et al., 1995).

Certain problems arise in attempting to quantify the level of hazard in low-seismicity areas using conventional probabilistic techniques such as the Cornell (1968) approach. The interpretation of earthquake observations in terms of faults and geologic structure is often difficult (e.g., Arvidsson and Kulhánek, 1994; Musson, 1997; Vetter et al., 1997). Also, there may not be enough data in each potential seismic source zone for a proper statistical estimation of the zone parameters. Their formal enlargement offers no solution, because too wide zones may give unreliable results (e.g., De Crook and Egozcue, 1992). Moreover, the historical events may have been reported quite incompletely. When destructive earthquakes are known to have occurred in the past their different interpretations influence the output for seismic hazard assessment (Grünthal and Bosse, 1997). Also, the attenuation law tends to remain inaccurate because of the limited number of earthquakes. Thus, it is specific for PSHA in low-seismicity areas that the small amount of data increases the level of personal judgement in the analysis (De Crook et al., 1989).

In the light of the above experiences, the new methodology proposed by Kijko and Graham (1998, 1999) offers interesting features for PSHA for low-seismicity regions, although its use is by no means limited only to such cases. It can be classified as parametric-historic because it combines the best features of the deductive (Cornell, 1968) and historical (Veneziano et al., 1984) procedures, which represent two main categories of PSHA methods (cf. McGuire, 1993). The new technique does not rely on the subjective judgement involved in the definition of seismic source zones, when specific active faults have not been identified. It permits the use of both the incompletely reported pre-instrumental and complete instrumental data and takes into account magnitude uncertainty. Either peak ground acceleration, peak ground velocity or peak ground displacement can be selected as the ground motion descriptor. The technique has been developed specifically for the estimation of seismic hazard at individual sites, but hazard maps can be created by applying it repetitively to grid points covering larger areas. In this study, the new methodology is outlined and applied to northernmost intraplate Europe. Seismic hazard parameters are estimated for a hypothetical engineering structure and a seismic hazard map is prepared for a subregion.

2. Seismic hazard assessment

The methodology is described in detail in Kijko and Graham (1998, 1999). The first part of their work is devoted to the investigation of statistical techniques which can be used for the evaluation of the maximum regional magnitude m_{max}. The different investigated procedures basically aim at correcting the bias of the classical maximum likelihood estimator equal to the maximum observed magnitude in the available catalogue. The main equations for those

estimators computed in the present study, namely the Kijko-Sellevoll estimator (cf. Kijko, 1983), abbreviated to K-S, and its Bayesian extension (K-S-B), are given below.

The K-S estimator for m_{max} has been derived for the doubly truncated Gutenberg-Richter relation, and it is computed according to the equation

$$\hat{m}_{max} = m_{max}^{obs} + \frac{E_1(Tz_2) - E_1(Tz_1)}{\beta \exp(-Tz_2)} + m_{min} \exp(-\lambda T), \tag{1}$$

where m_{max}^{obs} is the largest observed magnitude in the data covering time span T, m_{min} is the threshold magnitude for completeness of the data, beta is $\beta = b\ln 10$ with b being the b parameter of the Gutenberg-Richter relation and λ is the mean seismic activity rate; for abbreviation $z_1 = -\lambda A_1/(A_2 - A_1)$ and $z_2 = -\lambda A_2/(A_2 - A_1)$ with $A_1 = \exp(-\beta m_{min})$ and $A_2 = \exp(-\beta m_{max}^{obs})$. $E_1(\cdot)$ denotes an exponential integral function of the form

$$E_1(z) = \int_z^{\infty} \exp(-\zeta)/\zeta \, d\zeta. \tag{2}$$

The variance of the K-S estimator can be approximated as

$$Var(\hat{m}_{max}) \approx \sigma_M^2 + \left(\frac{E_1(Tz_2) - E_1(Tz_1)}{\beta \exp(-Tz_2)} + m_{min} \exp(-\lambda T) \right)^2. \tag{3}$$

Above, σ_M^2 is the variance of the random error in determination of the largest observed earthquake magnitude, and it is assumed to be known.

According to Kijko and Graham (1998) the Bayesian version of the estimator given in Eq. (1) becomes

$$\hat{m}_{max} = m_{max}^{obs} + \frac{\delta^{1/q+2} \exp[nr^q / (1 - r^q)]}{\beta} [\Gamma(-1/q, \delta r^q) - \Gamma(-1/q, \delta)]. \tag{4}$$

In Eq. (4), $\Gamma(\cdot,\cdot)$ denotes the incomplete gamma function having parameters p and q, $r = p/(p + m_{max}^{obs} - m_{min})$ and $\delta = n C_\beta$ with C_β being a normalizing coefficient of the form

$$C_\beta = [1 - (\frac{p}{p + m_{max}^{obs} - m_{min}})^q]^{-1}. \tag{5}$$

Eq. (5) is known as the Bayesian exponential-gamma cumulative distribution function (CDF) of earthquake magnitude.

The variance of the Bayesian estimator in Eq. (4) can be approximated as

$$Var(\hat{m}_{max}) \approx \sigma_M^2 + \left[\frac{\delta^{1/q+2} \exp[nr^q / (1 - r^q)]}{\beta} [\Gamma(-1/q, \delta r^q) - \Gamma(-1/q, \delta)] \right]^2. \tag{6}$$

The procedure for PSHA as proposed by Kijko and Graham (1998, 1999) consists of two steps. Firstly, the parameters maximum magnitude m_{max}, mean seismic activity rate λ and the Gutenberg-Richter b value, or $\beta = b\ln 10$, are computed for an area surrounding the specific site for which seismic hazard analysis is needed. The three parameters are determined simultaneously by an iterative scheme. Maximum magnitude m_{max} can be computed according to either Eq. (1) or Eq. (4), or some other relation given in Kijko and Graham (1998), whereas the evaluation of λ and β assumes the validity of a Poisson distribution of earthquake occurrence with activity rate λ and the doubly truncated Gutenberg-Richter magnitude-frequency relationship and employs the method of maximum likelihood (ML). When solving for the three hazard parameters simultaneously, it is possible to replace m_{max}^{obs} in Eqs. (1) and (4) by the value of m_{max}, where the first estimate of m_{max} can be equal to the value of m_{max}^{obs}. A continuous repetition of the solution scheme then uses the latest estimate of m_{max}, until convergence towards the exact value of m_{max} is obtained.

The area-specific parameters are estimated using all earthquake data available for the area of interest. In the model of a general earthquake catalogue as sketched already in Kijko and Sellevoll (1989, 1992), the data comprise two main parts, viz extreme and complete. In the extreme part the events have not been completely reported but are usually the largest ones only, while in the complete part the available data are complete above a certain threshold magnitude. The procedure also takes into account the uncertainty of the observed earthquake magnitudes and treats them as apparent values, which are the true, unknown magnitudes distorted by a random observation error (Tinti and Mulargia, 1985). Details of the numerical procedure for parameter estimation can be found in the original papers of Kijko and Sellevoll (1989, 1992).

The second step of computations for PSHA is site-specific (Kijko and Graham, 1999). This requires knowledge of the attenuation of the selected ground motion parameter a with distance. The attenuation law is assumed to be of the type

$$\ln(a) = c_1 + c_2 \cdot M + c_3 \cdot R + c_4 \cdot \ln(R) + \varepsilon, \tag{7}$$

where c_i, $i = 1,...,4$, are empirical coefficients, M denotes the earthquake magnitude, R is distance in km and ε is a normally distributed random error.

If peak ground acceleration (PGA) is chosen to describe ground motion, the parameters that characterize seismic hazard at a given site are site-specific λ_S, $\gamma = \beta/c_2$ and a_{max}, which is the maximum possible PGA at the site. The λ_S parameter is different from the area-specific lambda in the first step of computations: it refers to the activity rate of events that produce a PGA value a at the site exceeding a chosen threshold value a_{min} of engineering interest. It is assumed that the occurrence of events with PGA value a, $a \geq a_{min}$, at the site follows the Poisson distribution with a mean activity rate λ_S. Therefore the CDF of the logarithm of the largest PGA value x_{max} observed at the site during a given time interval t can be expressed as

$$F_X^{max}(x \mid x_{min}, x_{max}, t) = \frac{\exp\{-\lambda_S t[1 - F_X(x \mid x_{min}, x_{max})]\} - \exp(-\lambda_S t)}{1 - \exp(-\lambda_S t)}, \tag{8}$$

which is doubly truncated; from below, $x_{min} = \ln(a_{min})$, and from above, $m_{max} = \ln(a_{max})$. In Eq. (8), $\lambda_S(x) = \lambda_S\ [1 - F_X\ (x \mid x_{min},\ x_{max})]$, with $x = \ln(a)$, is the mean activity rate of the Poisson process describing the occurrence of earthquakes causing a PGA value a, $a \geq a_{min}$, at the site of interest.

The ML method is used to estimate the seismic hazard parameters. If the observations are $a_1,...,a_n$, that is the largest PGA values of n successive time intervals $t_1,...,t_n$ recorded at the site, then the likelihood function of the sample $x_1,...,x_n$, where $x_i = \ln(a_i)$, i = 1,...,n, for a specified a_{max} can be written as

$$L(\lambda,\gamma) = \prod_{i=0}^{n} f_X^{max}\ (x_i \mid x_{min}, x_{max}, t_i). \tag{9}$$

In Eq. (9), $f_X^{max}(x_i \mid x_{min}, x_{max}, t_i)$ is the probability density function of the logarithm of the largest PGA value observed at the site during a given time interval t. The ML estimators of parameters λ and γ can be determined by maximizing $L(\lambda,\gamma)$ under a condition that a relation for m_{max} is included, where parameter β is replaced by γ, λ by λ_S and m_{max}^{obs} is replaced by the logarithm of the maximum observed PGA $\ln(a_{max}^{obs})$. For a given value of x_{max}, maximizing Eq. (9) leads to solving two simultaneous equations. Details of the procedure are given in Kijko and Graham (1999).

3. Applications of the procedure to northern Europe

The outlined technique was applied to parts of northernmost intraplate Europe. In the first example seismic hazard parameters were estimated for a site of a hypothetical engineering structure (HES), and in the second a seismic hazard map was obtained by applying the procedure to grid points covering a larger area. The earthquake data were taken from an updated version of the FENCAT catalogue (Ahjos and Uski, 1992).

3.1. Example 1

This application was motivated by annual flooding of rivers along the western coast of Finland. The HES was a dam located at 64.3 °N and 24.5 °E (Fig. 1). The input data comprised the earthquakes reported within an area surrounding the HES at a maximum distance of about 350 km. The extreme part was taken to be the 356 events available for the time period between 1626 and 1964, and the remaining 472 earthquakes for the period from 1 January 1965 to 29 February 2000 constituted the complete part. The events in the extreme part were assigned size indicators using macroseismic parameters according to the macroseismic magnitude scale derived in Wahlström and Ahjos (1984) for this region, while the events in the complete part had instrumental local magnitudes. These two magnitude scales are compatible (Wahlström and Ahjos, 1984).

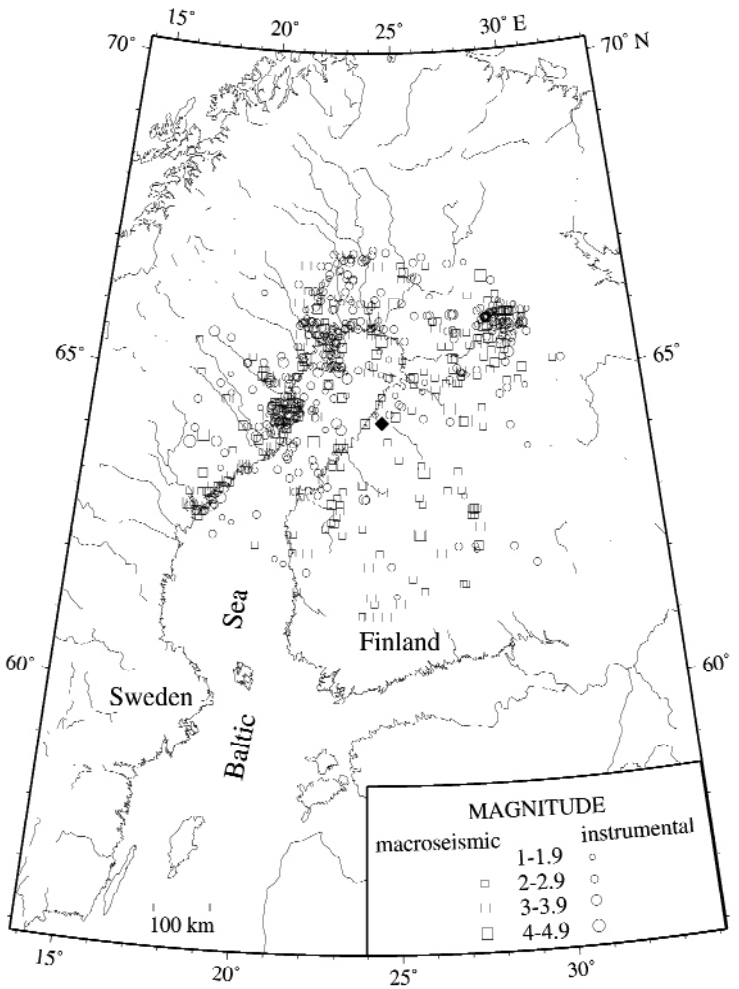

Fig. 1 - An illustration of the input data for example 1. The filled diamond marks the site of a hypothetical engineering structure located at (24.5 °E, 64.3 °N). Squares denote events between 1626 and 1964 whose size indicator is based on macroseismic information and circles events whose magnitudes are instrumental since 1965. Only events of macroseismic magnitude $M_M \geq 2$ and of instrumental magnitude $M_L \geq 1$ have been plotted. The two magnitude scales are compatible (see Wahlström and Ahjos, 1984).

Dependent events were removed from these data, and they were further subdivided into parts as follows: in the extreme part the standard deviation of the determination of magnitude was estimated at 0.5 magnitude units between 1626 and 1749, 0.4 between 1750 and 1880, 0.3 units between 1881 and 1959 and 0.2 between 1960 and 1964. The instrumental subcatalogues covered the years from 1965 to 1977, 1978 to 1989 and from 1990 to early 2000 with estimated thresholds of completeness equal to $M_L = 2.4$, $M_L = 2.1$ and $M_L = 1.7$, respectively.

These subdivisions of the data were based on changes in the earthquake data collection practices, which affect not only the quantity but also the level of accuracy of the observations. For example, the use of macroseismic questionnaires commenced in this region in the early 1880s, and improvements of the Finnish seismograph station network took place during 1977. The thresholds of completeness were estimated for the instrumental subcatalogues using cusum

charts, i.e. plots of the cumulative number of events as a function of the magnitude, assuming the validity of the linear Gutenberg-Richter magnitude-frequency relationship. The removal of dependent events was based on the experience obtained in Mäntyniemi (1996) for the Finnish data.

The largest earthquake known to have occurred within the investigated area was probably the event of 23 June 1882, whose macroseismic epicentre is located in the northern Baltic Sea inside Finnish territory. On the scale of Wahlström and Ahjos (1984), its macroseismic magnitude yields $M_M \approx 4.5$. A standard deviation equal to 0.5 magnitude units was used in computations for this event.

The main results of the area-specific part of the analysis are summarized in Fig. 2 and Table 1. Maximum magnitude was determined for the area of interest according to both the Kijko-Sellevoll and Kijko-Sellevoll-Bayes techniques. They gave quite similar results, close to the maximum observed magnitude, namely $\hat{m}_{max} = 4.56 \pm 0.50$ according to K-S equation and $\hat{m}_{max} = 4.53 \pm 0.50$ according to its Bayesian version. Fig. 2 shows the respective mean return times for this area. At magnitudes below 4.2 the two curves look alike but they deviate at the upper magnitude range, where the mean return time curve corresponding to the Bayesian technique bends more steeply. This has a noticeable effect on return times: according to the K-S approximation the return time for magnitude 4.5 is about 400 years with a standard deviation of around 20 years, while the Bayesian technique yields a return time of approximately 765 years with a standard deviation of over 40 years. Table 1 lists the

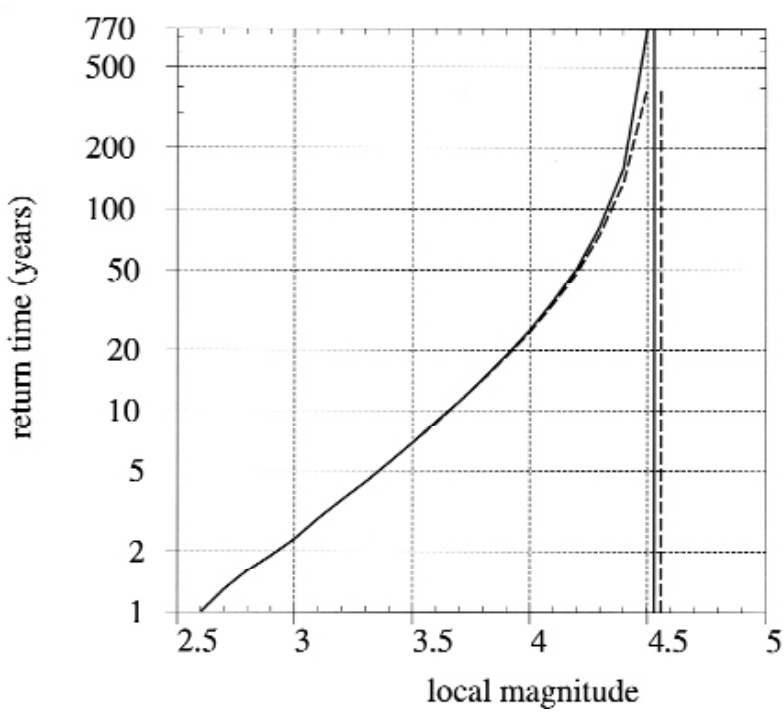

Fig. 2 - Mean return times for independent earthquakes in the area surrounding the hypothetical engineering structure of example 1. The estimated values for maximum magnitude m_{max} are also shown. The dashed line corresponds to the K-S estimator and the solid line to the K-S-B estimator (cf. section Seismic hazard assessment).

Table 1 - Probabilities that the given magnitudes will be exceeded in the area investigated in example 1 during one year, 50 years and 100 years. The values on the left were computed using the Kijko-Sellevoll (K-S) procedure and those on the right using the Kijko-Sellevoll-Bayes (K-S-B) approach (cf. section Seismic hazard assessment).

K-S				K-S-B		
Pr(T=1)	**Pr(T=50)**	**Pr(T=100)**	**Mag**	**Pr(T=1)**	**Pr(T=50)**	**Pr(T=100)**
0.1344	0.9993	0.9999	3.5	0.1343	0.9993	0.9999
0.1083	0.9968	0.9999	3.6	0.1080	0.9967	0.9999
0.0863	0.9890	0.9999	3.7	0.0859	0.9888	0.9999
0.0679	0.9703	0.9991	3.8	0.0674	0.9694	0.9991
0.0526	0.9329	0.9955	3.9	0.0519	0.9304	0.9952
0.0399	0.8691	0.9829	4.0	0.0390	0.8635	0.9814
0.0293	0.7738	0.9488	4.1	0.0284	0.7630	0.9438
0.0206	0.6460	0.8747	4.2	0.0196	0.6276	0.8613
0.0133	0.4892	0.7391	4.3	0.0123	0.4607	0.7091
0.0074	0.3103	0.5243	4.4	0.0063	0.2695	0.4663
0.0025	0.1181	0.2222	4.5	0.0013	0.0633	0.1226

probabilities that the values at the upper magnitude range available will be exceeded in the given time intervals. In accordance with the return times, the K-S-B technique gave lower probabilities than K-S. The *b* value obtained for the first, area-specific part of computations was $\hat{b} = 0.87 \pm 0.03$ (corresponding to $\hat{\beta} = 1.99 \pm 0.07$).

Maximum ground amplitude was chosen as the ground-motion descriptor for the next step of analysis, i.e. the site-specific hazard assessment. This has the advantage that more ample local data on which to base the attenuation curve are available; extremely sparse local acceleration data exist for the area in question. Moreover, in general terms, and bearing in mind the purpose of the exercise, ground-motion amplitude as such is useful and important as regards possible damage, whereas using acceleration to assess the exposure of buildings and other structures is quite problematic. The amplitude attenuation relation for the investigated area was taken from Uski and Tuppurainen (1996) and EMSC (1999). The average depth of earthquakes computed from the most reliable foci available was 8 km.

Fig. 3 displays the probabilities that a given maximum zero-to-peak amplitude will be exceeded at the HES site in time intervals equal to one year, 50 years and 100 years. The obtained site-specific lambda was $\hat{\lambda}_S \approx 0.35 \pm 0.02$ for amplitude greater than or equal to 100 μm. Results of example 1 are discussed further in section Conclusions.

3.2. Example 2

Earthquake epicentres falling inside the quadrant 55-70 °N and 10-33 °E were used as the input data for a seismic hazard map. This region covers most of the Fennoscandian Shield and northern Caledonides excluding western Norway (Fig. 4). The data available consisted of 1669

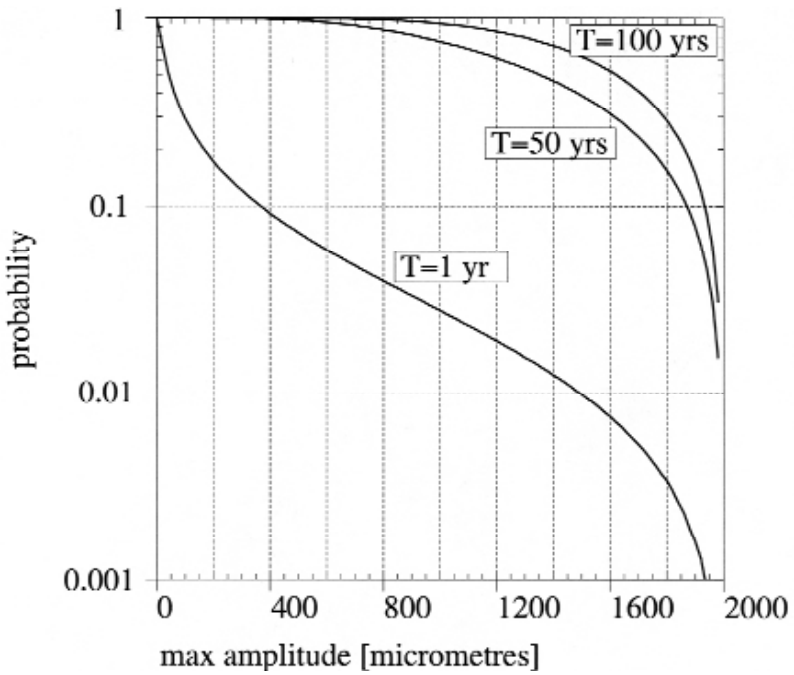

Fig. 3 - Probabilities that a given maximum zero-to-peak ground amplitude will be exceeded at the site of the hypothetical engineering structure of example 1 during time intervals equal to one year, 50 years and 100 years.

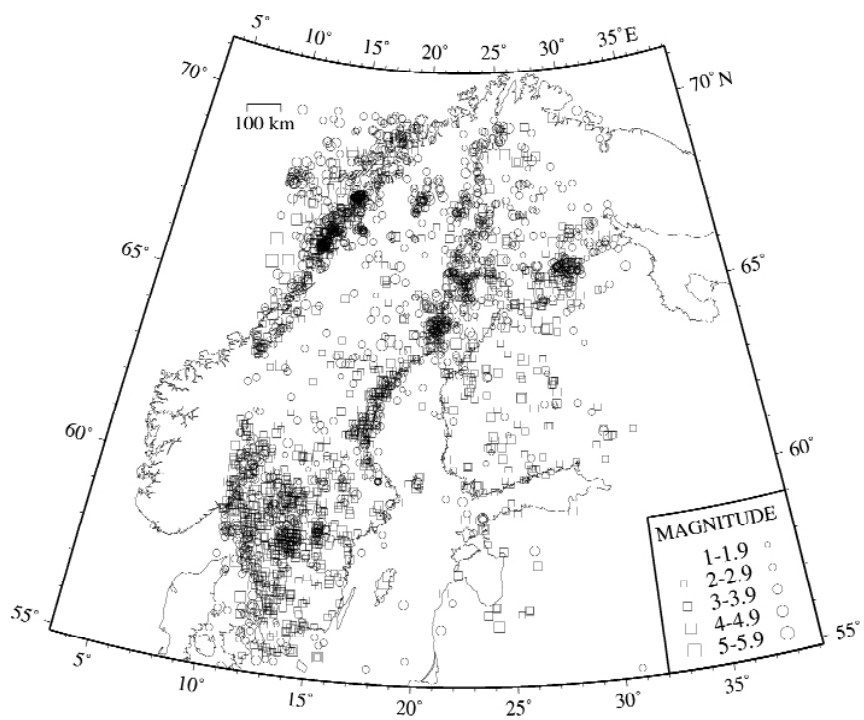

Fig. 4 - An epicentre map of the input data for example 2. Squares denote events between 1375 and 1964 whose size indicator is based on macroseismic information and circles events whose magnitudes are instrumental since 1965. Only events of macroseismic magnitude $M_M \geq 2$ and of instrumental magnitude $M_L \geq 1$ have been plotted.

events documented during the predominantly macroseismic era from 1375 to 1964 and 1877 earthquakes recorded instrumentally since 1965. They were arranged for computations in a similar way to example 1. The largest observation was the earthquake in northern Norway on 31 August 1819, which is also the largest known earthquake in all Fennoscandia (Ambraseys, 1985). Its magnitude as given in the FENCAT database was $M_S = 5.8$.

The available literature comprises some remarks as to the applicability of the Poisson distribution to these earthquake data. It is generally noted that the temporal distribution of seismicity in this region is non-Poissonian. This is commented upon for Swedish earthquake data in Kijko et al. (1993), for Norwegian data in Havskov et al. (1989), for Finnish data in Mäntyniemi (1996) and for the overall region in Mäntyniemi et al. (1993). When testing the Finnish data for a Poisson distribution, the testing procedure (the common χ^2 test) did not imply the rejection of these data following the Poisson distribution at the chosen significance levels even when the dependent events were included in the sample. In this case, however, the ratio of the variance to the mean exceeded unity, so the process was over-dispersed relative to the Poisson distribution. The closest fit to unity was obtained when a time-window equal to 5.5 days was used to identify dependent events (see Mäntyniemi, 1996, for more details). A time window equal to one week was used to identify and remove dependent events in the present study, as it is in reasonable agreement with the experiences reported in the literature.

The area-specific results yielded a b value equal to $\hat{b} = 0.84 \pm 0.01$. The maximum regional magnitude was $\hat{m}_{max} = 5.94 \pm 0.52$ obtained according to the K-S equation and $\hat{m}_{max} = 5.84 \pm 0.50$ according to the K-S-B equation, when the standard deviation in the determination of the largest observed magnitude was assigned at 0.5 magnitude units. Thus, the Bayesian version of the two equations yielded a lower value for m_{max}. The K-S technique gave a return time of 675 years with a standard deviation of about 20 years for magnitude 5.8 and a return time of 2600 years with a standard deviation of over 80 years for magnitude 5.9. According to the K-S-B equation, the return time for magnitude 5.8 was almost 2150 years with a standard deviation in excess of 70 years.

When applying the methodology repeatedly to sites corresponding to grid points, the attenuation coefficients were based on the table values provided by Atkinson and Boore (1995, 1997) and an average focal depth of 10 km was used. Fig. 5 illustrates seismic hazard maps for the chosen quadrant. They specify a 10% probability of exceedance of the given PGA values for an exposure time of 50 years. The grid size in the direction of longitude and latitude was 0.5 degrees.

4. Conclusions

In the present study, the level of seismic hazard originating from earthquakes was evaluated on the basis of knowledge of past seismicity. Seismic hazard was specified for a site of a hypothetical engineering structure and a seismic hazard map was created for a region covering a large part of the northernmost European intraplate. In both cases, the maximum magnitude m_{max} was estimated using two procedures. All the obtained values were rather close to the

respective maximum observed magnitude. This is in agreement with most of the cases presented in the earlier studies of Kijko et al. (1993) and Mäntyniemi et al. (1993), in which the K-S technique was applied to data from different subregions in northern Europe. Adequate uncertainties have to be assigned to these estimates, as the largest observations often stem from pre-instrumental parts of available catalogues.

The estimates for m_{max} obtained using the two techniques were also rather close to each other in both examples, and the K-S-B technique gave a lower value than the K-S one. The apparently rather minor differences between the estimates resulted in large deviations in the corresponding return times for the largest magnitudes. In numerical simulations, as reported in Kijko and Graham (1998), the K-S-B approach basically performed better than the K-S technique, and also the theoretical limitation of the K-S variance in Eq. (3) makes it best suited to large data sets of high-seismicity areas. In this study, however, no case for strong preference for either of these techniques can be made because all the computed return times exceed the span of the respective catalogue available.

In the first exercise, the procedure was applied to earthquake data within an area surrounding the hypothetical engineering structure at a selected distance. The choice of the distance affects the output if different distances mean different observations of the largest earthquakes, but otherwise the results for the area-specific part of computations are not that dependent on minor differences between chosen distances. In contrast, the site-specific lambda, λ_S, is quite sensitive to the number of observations utilized in computations. In both exercises, all available data were used to obtain the λ_S parameter. If only the earthquakes large enough to exceed a certain threshold value of engineering interest of the chosen ground-motion descriptor are considered, the remaining data are not very numerous. In such cases, a sound evaluation of seismic hazard for a site may not succeed, and the obtained seismic hazard maps tend to be dominated by the largest events. Computing the λ_S parameter on the basis of all available data may be seen as an adjustment of the methodology to the conditions in low-seismicity areas.

In the second example, one *b* value was used to characterize the whole region comprising different domains. A quite low *b* value was reported for northern Caledonides in Mäntyniemi et al. (1993), so the value used for the overall region has a somewhat formal character. Nevertheless, the created map shown in Fig. 5a gives rather a reasonable assessment of the level of seismic hazard, relying on the knowledge of past seismicity and the maximum effects documented during the last six centuries. The areas of more concentrated and quite scattered seismicity are discernible but the output is not dominated by the largest historical events as in the crudest hazard maps. A version of the seismic hazard map in which offshore areas are included is shown in Fig. 5b.

The maximum computed PGA value is $0.038g \approx 0.37$ m/s^2, which is reached along the coast of northern Norway. The highest obtained PGA values inside Swedish and Finnish territories are $0.022g \approx 0.22$ m/s^2 and $0.033g \approx 0.32$ m/s^2, respectively. In Finland, the maximum occurs in the Kuusamo area in the north, and this feature is quite pronounced, while in Sweden the computed maximum is reached both in the southern and northern parts of the country. These values do not differ very much from those displayed in some other probabilistic seismic hazard maps for this region. The map of Wahlström and Grünthal (2001) shows a maximum PGA value of the order

a)

b)

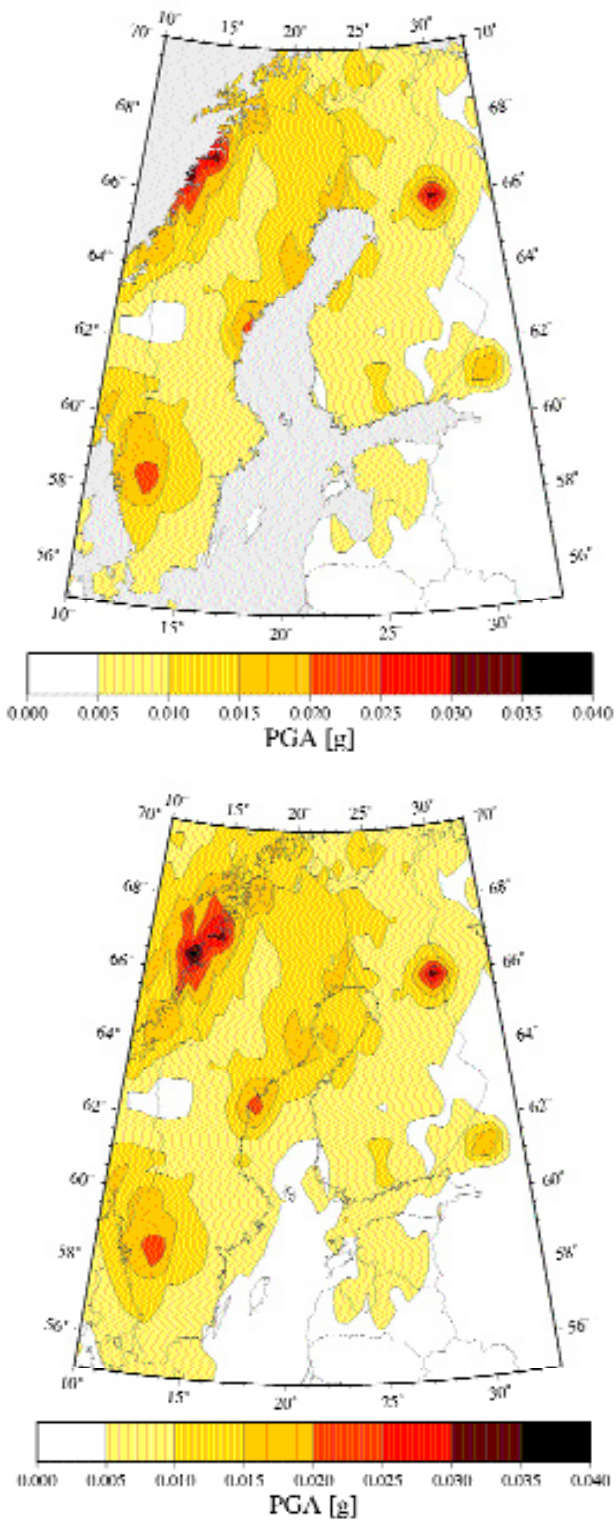

Fig. 5 - Seismic hazard maps plotted for a subregion of the northern European intraplate, specifying a 10% probability of exceedance of the given PGA values for an exposure time of 50 years. Offshore areas are excluded in Fig. 5a and included in Fig. 5b.

of 0.40-0.50 m/s^2 for the coastal area in northern Norway, corresponding to a return time of 475 years, and maximum PGA values in the range from 0.25 to 0.30 m/s^2 for the Kuusamo area in Finland, but their estimated PGA values for southern Sweden are higher than those presented in this map, namely between 0.30 and 0.35 m/s^2.

It is quite interesting to compare the spatial distribution of the hazard obtained using different methodologies. Wahlström and Grünthal (2000) used logic tree techniques based on regionalization and non-regionalization approaches, which gave somewhat different geographical distributions of the PGA isolines. The present map is more similar to the map based on the non-regionalization approach, but it also includes features shown only on the regionalization approch map, such as the enhanced seismicity of the Kuusamo area in Finland, which totally vanishes on the non-regionalization-approach map. The seismicity of Lake Ladoga at about 61°N and 31°E appears quite enhanced in the map, although the number of earthquake observations available for this area is rather small. This may in part be attributed to a group of events with identical epicentres originating from the macroseismic era, as location uncertainties may affect the λ_S parameter. Also the shape of the PGA isolines in the present map reflects some of the sensitivity of the λ_S parameter to the available observations.

Although no technique can of course compensate for the paucity of observations, several of the basic features of the methodology applied in this study serve very well in areas of low seismicity. The need to use all available seismicity information is well recognized but becomes more tangible when the available data are not numerous. The necessity to consider magnitude uncertainty is also not a novel remark but remains of the utmost importance especially because historical data are also considered. Not having to rely on the definition of seismogenic source zones is very favourable in these areas, which was demostrated especially for the Finnish territory, for which earlier seismic hazard maps do not comprise as many reasonable features as the present one. In short, the proposed methodology proved to be a useful tool for quantifying different aspects of seismic hazard in areas of low to moderate seismicity, and its main features are advantageous to these cases.

References

Adams J., Basham P.W. and Halchuk S.; 1995: *North-eastern North American earthquake potential - new challenges for seismic hazard mapping*. Geological Survey of Canada, Current Reseach 1995-D, 91-99.

Ahjos T. and Uski M.; 1992: *Earthquakes in northern Europe in 1375-1989*. Tectonophysics, **207**, 1-23.

Ambraseys N.N.; 1985: *The seismicity of western Scandinavia*. Earthquake Eng. Struct. Dyn., **13**, 361-399.

Arvidsson R. and Kulhánek O.; 1994: *Seismodynamics of Sweden deduced from earthquake focal mechanisms*. Geophys. J. Int., **116**, 377-392.

Atkinson G.M. and Boore D.M.; 1995: *Ground-motion relations for eastern North America*. Bull. Seism. Soc. Am., **85**, 17-30.

Atkinson G.M. and Boore D.M.; 1997: *Some comparisons between recent ground-motion relations*. Seism. Res. Lett., **68**, 24-40.

Cornell C.A.; 1968: *Engineering seismic risk analysis*. Bull. Seism. Soc. Am., **58**, 1583-1606.

Crook Th. de and Egozcue J.J.; 1992: *Comparison of two methods for seismic hazard assessment in a low-seismicity area*. Natural Hazards, **6**, 39-49.

Crook Th. de, Schenk V., Barbano M.S., Colombo F., Egozcue J.J., García-Fernández M., Kottnauer P., Leydecker G., Mantlík F., Schenková Z. and Zonno G.; 1989: *Seismic hazard computations for regions with low earthquake activity - a case study for the Belgium, The Netherlands and NW Germany area*. Natural Hazards, **2**, 229-236.

EMSC; 1999: Euro-Mediterranean Seismological Centre Newsletter, N° 15, 3 pp.

Giardini D. and Basham P.; 1993: *The global seismic hazard assessment program (GSHAP)*. Ann. Geofis., **36**, 3-13.

Grünthal G. and Bosse Ch.; 1997: *Seismic hazard assessment for low-seismicity areas - case study: Northern Germany*. Natural Hazards, **14**, 127-139.

Grünthal G. and the GSHAP Region 3 Working Group; 1999: *Seismic hazard assessment for Central, North and Northwest Europe: GSHAP Region 3*. Ann. Geofis., **42**, 999-1011.

Havskov J., Lindholm C.D. and Hansen R.A.; 1989: *Temporal variations in North Sea seismicity.* In: Gregersen S. and Basham P.W. (eds), Earthquakes at North-Atlantic passive margins: neotectonics and postglacial rebound, Kluwer, Dordrecht, pp. 413-427.

Kijko A.; 1983: *A modified form of the first Gumbel distribution: model for the occurrence of large earthquakes, Part II: Estimation of parameters*. Acta Geophys. Pol., **31**, 27-39.

Kijko A. and Graham G.; 1998: *Parametric-historic procedure for probabilistic seismic hazard analysis. Part I: Estimation of maximum regional magnitude* m_{max}. Pure Appl. Geophys., **152**, 413-442.

Kijko A. and Graham G.; 1999: *Parametric-historic procedure for probabilistic seismic hazard analysis. Part II: Assessment of seismic hazard at specified site*. Pure Appl. Geophys., **154**, 1-22.

Kijko A. and Sellevoll M.A.; 1989: *Estimation of earthquake hazard parameters from incomplete data files. Part I. Utilization of extreme and complete catalogs with different threshold magnitudes*. Bull. Seism. Soc. Am., **79**, 645-654.

Kijko A. and Sellevoll M.A.; 1992: *Estimation of earthquake hazard parameters from incomplete data files. Part II. Incorporation of magnitude heterogeneity.* Bull. Seism. Soc. Am., **82**, 120-134.

Kijko A., Skordas E., Wahlström R. and Mäntyniemi P.; 1993: *Maximum likelihood estimation of seismic hazard for Sweden*. Natural Hazards, **7**, 41-57.

Mäntyniemi P.; 1996: *Some features of Finnish earthquake data*. Geophysica, **32**, 273-289.

Mäntyniemi P., Wahlström R., Lindholm C. and Kijko A.; 1993: *Seismic hazard in Fennoscandia: a regionalized study*. Tectonophysics, **227**, 205-213.

McGuire R.K.; 1993: *Computations of seismic hazard*. Ann. Geofis., **36**, 181-200.

Musson R.M.W.; 1997: *Seismic hazard studies in the U.K.: source specification problems of intraplate seismicity.* Natural Hazards, **15**, 105-119.

Tinti S. and Mulargia F.; 1985: *Effects of magnitude uncertainties on estimating the parameters in the Gutenberg-Richter frequency-magnitude law.* Bull. Seism. Soc. Am., **75**, 1681-1697.

Uski M. and Tuppurainen A.; 1996: *A new local magnitude scale for the Finnish seismic network*. Tectonophysics, **261**, 23-37.

Veneziano D., Cornell C.A. and O'Hara T.; 1984: *Historic method of seismic hazard analysis*. In: Rep. NP-3438, Elect. Power Res. Inst., Palo Alto, California.

Vetter U.R., Ake J.P. and Laforge R.C.; 1997: *Seismic hazard evaluation for dams in northern Colorado, U.S.A.*. Natural Hazards, **14**, 227-240.

Wahlström R. and Ahjos T.; 1984: *Magnitude determination of earthquakes in the Baltic Shield*. Ann. Geophys., **2**, 553-558.

Wahlström R. and Grünthal G.; 2000: *Probabilistic seismic hazard assessment (horizontal PGA) for Sweden, Finland and Denmark using different logic tree approaches*. Soil Dynamics and Earthquake Engineering, **20**, 45-58.

Wahlström R. and Grünthal G.; 2001: *Probabilistic seismic hazard assessment (horizontal PGA) for Fennoscandia using the logic tree approach for regionalization and nonregionalization models*. Seism. Res. Lett., **72**, 33-45.